Brain and Spine 4 (2024) 102671

Contents lists available at ScienceDirect

Brain and Spine

journal homepage: www.journals.elsevier.com/brain-and-spine

# Radiological characterization of pediatric intramedullary astrocytomas: Do they differ from adults?

Nathalie Gilis [a,*,1], Laetitia Lebrun [b,1], Valentina Lolli [c], Philippe David [c], Marine Rodesch [d], Alix Bex [a], Christophe Fricx [d], Vivianne De Maertelaer [e], Isabelle Salmon [b,2], Olivier De Witte [a,2]

[a] Department of Neurosurgery, Erasmus Hospital, Route de Lennik 808, Brussels, Belgium
[b] Department of Pathology, Erasmus Hospital, Route de Lennik 808, Brussels, Belgium
[c] Department of Radiology, Erasmus Hospital, Route de Lennik 808, Brussels, Belgium
[d] Department of Pediatrics, Erasmus Hospital, Route de Lennik 808, Brussels, Belgium
[e] Institute of Interdisciplinary Research (IRIBHM), Université Libre de Bruxelles, Route de Lennik 808, Brussels, Belgium

ARTICLE INFO

*Keywords:*
Intramedullary astrocytoma
Pediatric spinal cord tumor
Pilocytic astrocytoma

ABSTRACT

*Introduction:* The incidence of intramedullary spinal cord tumors ranges from 2 to 4% of all central nervous system tumors. Only 6–8% are astrocytomas. The gold standard to diagnose a spinal cord tumor is the spinal cord MRI *in toto*. Specific radiological criteria orient the diagnosis of the intradural intramedullary lesion. Most of the authors studied adult populations of astrocytomas. However, pediatric astrocytomas present certain particularities.
*Research question:* This work aims to determine if the usual radiological criteria of intramedullary astrocytomas (IMAs) are different depending on the patient's age.
*Material & methods:* We evaluated the radiological features of IMAs in adult and pediatric groups through a retrospective study.
*Results:* We collected 31 patients with IMAs (11 children and 20 adults). We observed some trends but we did not highlight any statistically significant difference between all the radiological criteria studied (sagittal and axial spinal cord localization, T1-and T2-weighted characteristics, contrast uptake, infiltrating character, presence of necrosis, heterogeneous lesion, necrotic, hemorrhagic, presence of edema) and the patient's age.
*Discussion & conclusion:* Given the rarity of IMAs and the lack of large specific pediatric studies, it seems essential to routinely report all cases encountered and create multicentric pediatric databases to draw more robust conclusions.

## 1. Introduction

The incidence of intramedullary spinal cord tumors ranges from 2 to 4% of all central nervous system tumors. About 80% of these tumors belong to the group of glial tumors. Most (60–70%) of glial tumors are ependymomas, and astrocytomas are encountered in approximately 30–40% of cases (Ogunlade et al.; Campello et al., 2021; Lebrun et al., 2020; Knafo et al., 2021; Parker et al., 2017). According to estimates, 6–8% of all spinal cord tumors (extradural, intradural extramedullary, or intramedullary) are astrocytomas (Ogunlade et al.).

Intramedullary astrocytomas (IMAs) can be classified into low and high grades. Low-grade astrocytomas include grade 1 astrocytomas (pilocytic astrocytomas) and grade 2 astrocytomas (diffuse astrocytomas), while high-grade astrocytomas include grade 3 (anaplastic astrocytomas) and grade 4 astrocytomas (glioblastoma). According to molecular analysis, diffuse midline gliomas found in the thalamus, brainstem, and spinal cord are high-grade astrocytomas presenting mutations in H3 histones gene (*H3F3A, HIST1H3B/C*) and behave similarly to glioblastomas (Campello et al., 2021; Lebrun et al., 2020; Louis et al., 2016; Gessi et al., 2015).

The gold standard to diagnose a spinal cord tumor is the spinal cord MRI *in toto*. Specific radiological criteria orient the diagnosis of IMA

* Corresponding author. Route de Lennik, 808, 1070, Brussels, Belgium.
*E-mail address:* nathalie.gilis@hubruxelles.be (N. Gilis).
[1] These authors contributed equally to the manuscript as co-first authors.
[2] These authors contributed equally to the manuscript as co-promotors.

https://doi.org/10.1016/j.bas.2023.102671
Received 10 May 2023; Received in revised form 28 August 2023; Accepted 5 September 2023
Available online 7 September 2023

(Fig. 1). Indeed, IMAs are frequently encountered at the thoracic level extending over several vertebral bodies; these are eccentric, poorly delimited lesions that may be associated with cysts. On T1-weighted imaging, these lesions appear iso- or hypo-intense, while on T2-weighted images, they appear hyper-intense. After gadolinium injection, contrast uptake is significant and heterogeneous. The degree of this contrast enhancement is unrelated to tumoral aggressiveness, in contrast to cerebral glial lesions (Ogunlade et al.; Campello et al., 2021; Knafo et al., 2021; Parker et al., 2017; Seo et al., 2010; Marrazzo et al., 2021; Do-Dai et al., 2010; Bourgouin et al., 1998).

Most of the authors reporting these characteristics have studied adult populations of astrocytomas. However, pediatric IMAs present certain particularities. For example, sharper tumor margins are more common in pediatric low-grade astrocytomas than in adults. They preferentially sit at the cervical or cervicothoracic junction rather than at the thoracic level (Marrazzo et al., 2021; Houten and Weiner, 2000) and about 70% of pediatric pilocytic astrocytomas show significant enhancement after contrast injection. This raises the question of the validity of these "typical" radiological criteria in a pediatric population.

This work aims to determine if the usual radiological criteria of intramedullary astrocytomas differ depending on the patient's age.


**Fig. 1.** 12-year-old girl with a medullary pilocytic astrocytoma. A. Sagittal T2-WI; B. Sagittal post-gadolinium T1-WI; C. Axial post-gadolinium T1-WI; D. Axial T2*-WI). MRI of the spinal cord reveals an intramedullary tumor mass extending from the inferior aspect of C4 to the upper part of Th1. There is expansion of the dural canal and moderate bone scalloping. The lesion shows increased SI on T2- (A) and T2* (D) -WI and marked peripheral enhancement (B, C). There is marked T2 prolongation below and above the tumoral mass indicating vasogenic edema (A)
Legend: WI = weighted image; SI = signal intensity.

## 2. Materials & methods

### 2.1. Study design

After approval by our local ethics committee (Erasmus hospital with reference P2017/319), we conducted a retrospective study on patients operated for an intramedullary astrocytoma in the Neurosurgical Department of Erasmus hospital between 1989 and 2019. We included patients who benefited from a preoperative MRI scan, whose anatomopathological sampling was carried out by the Department of Pathology of Erasmus hospital, and who did not indicate their refusal to participate in a clinical study. Demographic data were collected as well as anatomopathological diagnoses and radiological characteristics. A patient was defined as an adult if they were older than 18. Patients were excluded when imaging data was not available anymore, when the patient was not operated by our team and when the samples were not analyzed within our institution.

### 2.2. Pathological examination and molecular analyses

Pathological diagnosis was reviewed by 2 pathologists (L.L. and S.I.) according to the WHO 2021 classification (Louis et al., 2016), as previously described (Lebrun et al., 2020). Molecular profiles were obtained by using 2 AmpliSeq gene-targeted DNA custom panels ("Clinical Glioma" and "Research Glioma" panels) and a specific KIAA1549-BRAF fusion panel, as previously described (Lebrun et al., 2020). These 3 panels analyzed a total of 33 genes commonly implicated in gliomas, the 1p and 19q regions and 10 different KIAA1549-BRAF fusions described in the COSMIC database (Sanger Institute Catalog of Somatic Mutations in Cancer).

### 2.3. Radiological work-up

Patients who underwent preoperative MRI, including at least T1-and T2-weighted sagittal and axial acquisitions and post-gadolinium T1-weighted images, were included. An experienced neuroradiologist (L.V. or D.P.) reviewed the images. The following radiological characteristics were assessed: the intramedullary location of the lesion in the sagittal plane (cervical, cervicothoracic, thoracic, thoracolumbar region, or lumbar level) and in the axial plane (central, lateral or all-width), the features on T1-and T2-weighted images (hypo-, hyper-, iso-signal or a mixed-signal), contrast uptake following gadolinium injection, tumoral margins (infiltrative or well-defined), presence of specifics characteristics (homogeneous structure, solid, cystic and/or necrotic component, calcifications, bleeding or edema surrounding the lesion). The resection rates were classified into four categories: biopsy, partial resection, near total resection, and total resection. The resection is qualified as total resection when there was no residue left, as near total resection when resection was at least 90% of the initial mass, and a partial resection for other degrees of resection.

## 3. Statistical analysis

The continuous variables are summarized by their means and standard deviations, and the categorical variables by their frequencies and percentages. Associations between categorical variables are analyzed using Pearson's Chi-Squared tests. Statistical tests are significant when the corresponding p-value is less than 0,05. Statistical tests were performed using IBM-SPSS® version 28.0 software.

## 4. Results

### 4.1. Demographic data

Table 1 provides the cohort's demographic characteristics. In the reference period, we collected 52 patients with an IMA. From the 52 patients, 21 were excluded of which four due to the lack of available preoperative MRI scans; 17 patients benefited from a follow-up in our institution but were not operated on by us. There were 31 patients in total meeting all inclusion criteria. This cohort included 11 children and 20 adults. The mean age for children was 11,71 years (with a range from 7 to 18) while the mean for adults was 39,71 (range from 20 to 61). In our cohort, the female population represented 38,7% of cases.

**Table 1**
Demographical data.

| | | N = | Percentage (%) |
|---|---|---|---|
| Number of patients | | 31 | 100 |
| | *pediatric population | 11 | 35,5 |
| | *adult population | 20 | 64,5 |
| Gender: Female | | 12 | 38,7 |
| | | Means ± standard deviations | |
| Age (in years) | *pediatric population | 11,71 ± 3,99 | |
| | *adult population | 39,71 ± 13,51 | |

### 4.2. Pathological results

Table 2 shows the distribution of pathological diagnoses over the global cohort and stratified by age category. In our cohort, the majority (N = 26/31, 84%) of IMAs are low-grade tumors, of which nearly 40% are pilocytic astrocytomas, and about one-third (N = 11) are grade 2 astrocytomas. All of the high grade astrocytomas (N = 5/31, 16%) harboured *H3F3A* K27M mutations leading to the diagnosis of Diffuse Midline Glioma, H3K27M-altered 16% of our diagnoses. The most frequent pathology in children was the pilocytic astrocytoma (N = 5/11, 45,4%) while it was grade 2 astrocytoma for their adult counterparts (N = 9/20, 45%). On the other hand, high grade IMAs was found in 27,3% of children and 10% of the adult cohort.

Pearson's Chi-squared test crosses the anatomopathological diagnosis and the patient's age (adult versus pediatric population). Our results show a value of 2958 (p-value = 0,451), suggesting a lack of statistical significance difference between the distribution of different tumor entities according to the age of the patients.

### 4.3. Radiological results

All radiological variables (characteristics of the T1-and T2-weighted images, localization in the sagittal and axial planes, contrast uptake, tumoral margins, heterogeneous components: solid, cystic, necrosis, calcification, or intralesional hemorrhage) were analyzed according to Pearson's Chi-Squared tests and p-values were calculated. There was no statistical difference between our pediatric and adult groups for any studied variables. The results are summarized in Table 3.

Despite the fact that there was no significant difference between children and adults in our overall IMAs' cohort, we did notice some

**Table 2**
Pathological data.

| | Global Cohort | | Pediatric Population | | Adult Population | |
|---|---|---|---|---|---|---|
| | N = | Percentage (%) | N = | Percentage (%) | N = | Percentage (%) |
| Pilocytic Astrocytoma | 12 | 38,7 | 5 | 45,4 | 7 | 35 |
| Grade 2 Astrocytoma | 11 | 35,5 | 2 | 18,2 | 9 | 45 |
| Low grade Astrocytoma | 3 | 9,7 | 1 | 9,1 | 2 | 10 |
| Grade 3 Astrocytoma | 0 | 0 | 0 | 0 | 0 | 0 |
| DMG H3K27M | 5 | 16,1 | 3 | 27,3 | 2 | 10 |
| TOTAL | 31 | 100 | 11 | 100 | 20 | 100 |

**Table 3**
Radiological characteristics and Pearson's Chi-Squared test results.

| Variables | | Population: | | | | | | Chi-Squared Test | |
|---|---|---|---|---|---|---|---|---|---|
| | | Global cohort (N = 31) | | Pediatric (N = 11) | | Adult (N = 20) | | (pediatric vs adult population) | |
| | | N = | % | N = | % | N = | % | Results | p values |
| T1-weighted images | | | | | | | | 5415 | 0,379 |
| | hypointense | 10 | 32,3 | 5 | 45,5 | 5 | 25,0 | | |
| | hyperintense | 14 | 45,2 | 4 | 36,4 | 10 | 50,0 | | |
| | isointense | 3 | 9,7 | 0 | 0 | 3 | 15,0 | | |
| | isointense + hypointense | 1 | 3,2 | 1 | 9,1 | 0 | 0,0 | | |
| | isointense + hyperintense | 2 | 6,5 | 1 | 9,1 | 1 | 5,0 | | |
| | hypointense + hyperintense | 1 | 3,2 | 0 | 0 | 1 | 5,0 | | |
| T2-weighted images | | | | | | | | 3785 | 0,301 |
| | hypointense | 5 | 16,1 | 3 | 27,3 | 2 | 10,0 | | |
| | hyperintense | 22 | 71,0 | 6 | 54,5 | 16 | 80,0 | | |
| | isointense | 1 | 3,2 | 0 | 0 | 1 | 5,0 | | |
| | hypointense + hyperintense | 3 | 9,7 | 2 | 18,2 | 1 | 5,0 | | |
| Localization in the sagittal plane | | | | | | | | 5058 | 0,278 |
| | Cervical | 11 | 35,5 | 3 | 27,3 | 8 | 40,0 | | |
| | Cervicothoracic | 10 | 32,3 | 6 | 54,5 | 4 | 20,0 | | |
| | Thoracic | 7 | 22,6 | 1 | 9,1 | 6 | 30,0 | | |
| | Thoracolumbar | 2 | 6,5 | 1 | 9,1 | 1 | 5,0 | | |
| | Lumbar | 1 | 3,2 | 0 | 0 | 1 | 5,0 | | |
| Localization in the axial plane | | | | | | | | 4742 | 0,098 |
| | Central | 3 | 9,7 | 0 | 0 | 3 | 15,0 | | |
| | Lateral | 18 | 58,1 | 5 | 45,5 | 13 | 65,0 | | |
| | All-width | 10 | 32,3 | 6 | 54,5 | 4 | 20,0 | | |
| Contrast Uptake | | | | | | | | 3279 | 0,133 |
| | No | 5 | 16,1 | 0 | 0,0 | 5 | 25,0 | | |
| | Yes | 26 | 83,9 | 11 | 100,0 | 15 | 75,0 | | |
| Contrast Uptake Homogeneity | | | | | | | | 2526 | 0,269 |
| | Homogeneous | 4 | 12,9 | 0 | 0,0 | 4 | 20,0 | | |
| | Heterogeneous | 27 | 87,1 | 11 | 100,0 | 16 | 80,0 | | |
| Tumoral Margins | | | | | | | | 3161 | 0,177 |
| | Well-defined | 11 | 35,5 | 2 | 18,2 | 10 | 50,0 | | |
| | Infiltrative | 19 | 61,3 | 9 | 81,8 | 10 | 50,0 | | |
| Heterogenous Lesion | | | | | | | | 0,624 | 0631 |
| | Yes | 26 | 83,9 | 10 | 90,9 | 16 | 80,0 | | |
| | No | 5 | 16,1 | 1 | 9,1 | 4 | 20,0 | | |
| Solid Component | | | | | | | | 1879 | 0,355 |
| | Yes | 30 | 96,8 | 10 | 90,9 | 20 | 100,0 | | |
| | No | 1 | 3,2 | 1 | 9,1 | 0 | 0,0 | | |
| Cystic Component | | | | | | | | 0,189 | 1 |
| | Yes | 24 | 77,4 | 9 | 81,8 | 15 | 75,0 | | |
| | No | 7 | 22,6 | 2 | 18,2 | 5 | 25,0 | | |
| Necrosis | | | | | | | | 1853 | 0,21 |
| | Yes | 7 | 22,6 | 4 | 36,4 | 3 | 15,0 | | |
| | No | 24 | 77,4 | 7 | 63,6 | 17 | 85,0 | | |
| Calcifications & intralesional hemorrhages | | | | | | | | 0,059 | 1 |
| | Yes | 16 | 51,6 | 6 | 54,5 | 10 | 50,0 | | |
| | No | 15 | 48,4 | 5 | 45,5 | 10 | 50,0 | | |
| Perilesional edema | | | | | | | | 0,94 | 0,452 |
| | Yes | 12 | 38,7 | 3 | 27,3 | 9 | 45,0 | | |
| | No | 19 | 61,3 | 8 | 72,7 | 11 | 55,0 | | |

Statistical signification: P value < 0,05.

trends. In T2-weighted imaging, our adult group shows hyperintense behavior more frequently (80% vs 54,5%) than in youngsters. The cervicothoracic junction is where most lesions in children are found (54,5%), whereas upper cervical lesions are more prevalent among the elderly. In contrast to adults, who have an axial distribution of IMAs that is almost lateralized (65% of cases) almost half of children presents an IMA invading the entire spinal cord width. Only 50% of adult IMAs are infiltrative, compared to 81,8% of their pediatric counterparts.

Table 4 provides data about our specific population of pilocytic astrocytomas (PA). Several characteristics in T1-and T2-weighted images, the sagittal localization of PA, the tumor margins, and the presence of perilesional edema seem to differ between our populations of children and adults (Fig. 2). We observe that the pediatric population of PAs appears mostly hypointense (60%) in T1-weighted images, whereas the adult population is mainly hyperintense (71,4%). Another difference appears in T2-weighted images, where only 20% of children show an hypersignal compared to 57,1% of adults. Interestingly, 80% of pediatric PAs are found in the cervicothoracic region, a localization which is never observed in our adult population. As noticed in our overall cohort (Table 3), tumoral margins in children are infiltrative compared to adults where they appear mostly well-defined. Surprisingly, 85,7% of adults PAs showed perilesional edema, whereas 80% of the children in our cohort did not show any edema.

Resection rates are detailed on Table 5. In our series, we observed

**Table 4**
Radiological Results detailed for pilocytic astrocytoma (pediatric versus adult population).

| Pilocytic Astrocytoma | | Population: | | | |
|---|---|---|---|---|---|
| Variables | | Pediatric (N = 5) | | Adult (N = 7) | |
| | | N = | % | N = | % |
| T1-weighted images | | | | | |
| | hypointense | 3 | 60 | 1 | 14,3 |
| | hyperintense | 1 | 20 | 5 | 71,4 |
| | isointense | 0 | 0 | 0 | 0,0 |
| | isointense + hypointense | 0 | 0 | 0 | 0,0 |
| | isointense + hyperintense | 1 | 20 | 0 | 0,0 |
| | hypointense + hyperintense | 0 | 0 | 1 | 14,3 |
| T2-weighted images | | | | | |
| | hypointense | 2 | 40 | 2 | 28,5 |
| | hyperintense | 1 | 20 | 4 | 57,1 |
| | isointense | 0 | 0 | 1 | 14,3 |
| | hypointense + hyperintense | 2 | 40 | 0 | 0,0 |
| Localization in the sagittal plane | | | | | |
| | Cervical | 1 | 20 | 3 | 42,8 |
| | Cervicothoracic | 4 | 80 | 0 | 0,0 |
| | Thoracic | 0 | 0 | 3 | 42,8 |
| | Thoracolumbar | 0 | 0 | 1 | 14,3 |
| | Lumbar | 0 | 0 | 0 | 0,0 |
| Localization in the axial plane | | | | | |
| | Central | 0 | 0 | 1 | 14,3 |
| | Lateral | 3 | 60 | 6 | 85,7 |
| | All-width | 2 | 40 | 0 | 0,0 |
| Contrast Uptake | | | | | |
| | No | 0 | 0,0 | 0 | 0,0 |
| | Yes | 5 | 100,0 | 7 | 100,0 |
| Contrast Uptake Homogeneity | | | | | |
| | Homogeneous | 0 | 0,0 | 1 | 14,3 |
| | Heterogeneous | 5 | 100,0 | 6 | 85,7 |
| Tumoral Margins | | | | | |
| | Well-defined | 1 | 20 | 4 | 57,1 |
| | Infiltrative | 4 | 80 | 3 | 42,8 |
| Heterogenous Lesion | | | | | |
| | Yes | 5 | 100 | 6 | 85,7 |
| | No | 0 | 0 | 1 | 14,3 |
| Solid Component | | | | | |
| | Yes | 4 | 80 | 7 | 100,0 |
| | No | 1 | 20 | 0 | 0,0 |
| Cystic Component | | | | | |
| | Yes | 5 | 100 | 5 | 71,4 |
| | No | 0 | 0 | 2 | 28,5 |
| Necrosis | | | | | |
| | Yes | 1 | 20 | 1 | 14,3 |
| | No | 4 | 80 | 6 | 85,7 |
| Calcifications & intralesional hemorrhages | | | | | |
| | Yes | 5 | 100 | 6 | 85,7 |
| | No | 0 | 0 | 1 | 14,3 |
| Perilesional edema | | | | | |
| | Yes | 1 | 20 | 6 | 85,7 |
| | No | 4 | 80 | 1 | 14,3 |

that gross total resection was achieved for PAs in adult patients only, as the majority of children with PAs underwent partial resection. This might be explained by the fact that in adults, we observed the presence of edema more frequently than in children. Technically, the presence of perilesional edema may help the surgeon to find a better cleavage plane between the PA and the medullary parenchyma.

## 5. Discussion

### 5.1. Results

Intramedullary astrocytomas are rare central nervous system tumors which require expertise for their management. The radiological workup is the first crucial step.

IMAs are typically described as heterogeneous lesions of the thoracic spinal cord, eccentric, poorly demarcated, often hypo- or iso-intense on T1-weighting images and enhanced after injection of contrast. As compared to these typical characteristics (Ogunlade et al.; Campello et al., 2021; Knafo et al., 2021; Parker et al., 2017; Seo et al., 2010; Marrazzo et al., 2021; Do-Dai et al., 2010; Bourgouin et al., 1998), the IMAs in our cohort differ in two aspects: their intramedullary locations in the sagittal plane and their T1-weighted characteristics. Indeed, the population of astrocytomas that we studied seat 35,5% at the cervical level, 32,3% at the cervicothoracic junction, and 22,6% at the thoracic level. We observed that IMAs mainly present a hyper signal in T1-and T2-weighted images, which could be related to the necrosis rates found in our cohort. In fact, in our series, 22,6% of IMAs presented a necrotic component, which contrasts with the reported observations of 3% necrosis by Parker et al. (2017). One explanation could be that our series has twice as many (16,1% versus 8%) grade 4 gliomas as the French series. However, Hachicha et al. (2021) reported that high-grade astrocytomas present a higher necrosis rate than low-grade ones.

Regarding the pediatric population, we did not highlight any statistically significant difference between all the radiological criteria studied (sagittal and axial spinal cord localization, T1-and T2-weighted characteristics, contrast uptake, infiltrating character, presence of necrosis, heterogeneous lesion, necrotic, hemorrhagic, presence of edema) and the age of the patients. This absence of difference could be explained by the small number of pediatric patients enrolled (eleven) compared to the adult population (twenty). In the literature, IMAs in children are most frequently low-grade astrocytomas. Compared to the adult population, they tend to be located at the cervical or cervicothoracic junction rather than at the thoracic level (Marrazzo et al., 2021; Houten and Weiner, 2000). Our observations point in the same direction with pediatric pilocytic astrocytomas occurring for 80% of our cases at the cervicothoracic junction and 20% at the upper cervical region. In contrast, 57,1% of adults PAs were observed at the thoracic level or below. Our observations suggest that adults PA are frequently associated with edema but not in the pediatric population. This observation should be confirmed by larger series but it raises the question of the underlying pathophysiology. A hypothesis could be that the mass effect of lesions arising from the cervical bulge compared to those within the thoracic spine could compress the spinal cord more tightly and cause more edema, particularly in the case of hemorrhage.

Given the rarity of intramedullary astrocytomas and the lack of large pediatric studies, it seems essential to routinely report all cases encountered and create multicentric pediatric databases to draw more robust conclusions.

### 5.2. Limitations

Our study has a retrospective design and therefore suffers from limitations related to this kind of data collection.

The size of our pediatric sample could influence the lack of statistical significance observed.

The introduction of the new 2021 WHO nomenclature for central nervous system tumors revises the anatomopathological classification of tumors; certain entities of our cohort, given further molecular or epigenetic analyses, could be classified differently. However, it is currently impossible to carry out new analyses and retrospectively revise the anatomopathological diagnoses based on the 2016 WHO classification, due to the small size and availability of tumor samples.

These observations advocate for multicentric prospective studies to centralize radiological and anatomopathological data about pediatric intramedullary astrocytomas.

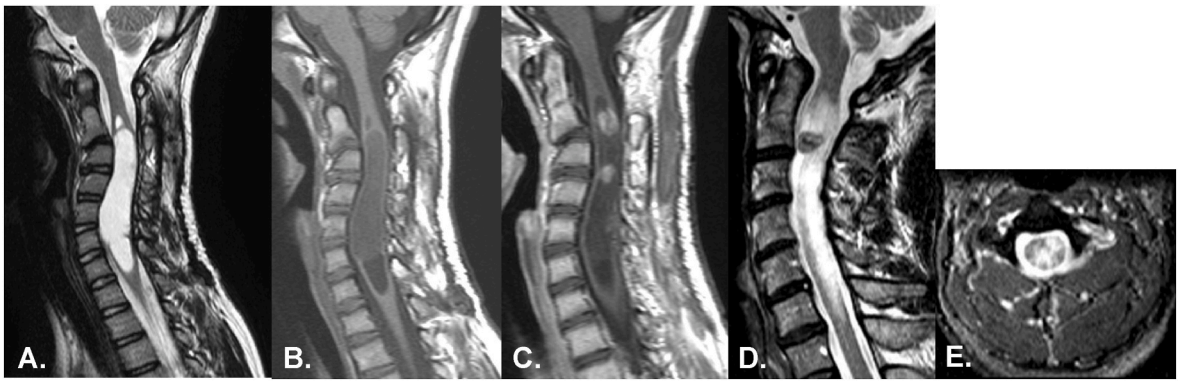


**Fig. 2.** Comparison of pediatric and adult pilocytic astrocytomas. A. and D. Sagittal T2-WI. B. Sagittal T1-WI. C. Sagittal post-gadolinium T1-WI. E. Axial T2-WI. Pediatric case: MRI reveals an intramedullary tumor mass with multiple cysts extending from C2 to C7 without any surrounding edema (A, B). The solid component of the astrocytoma shows contrast enhancement (C). Adult case: MRI demonstrates extensive vasogenic edema surrounding the pilocytic astrocytoma extending from C2 to C7 on sagittal and axial planes (D, E).
Legend: WI = weighted image.

**Table 5**
Surgical resection rates.

| Kind of surgery | Diagnosis | Population: | | | | | |
|---|---|---|---|---|---|---|---|
| | | Global cohort (N = 31) | | Pediatric (N = 11) | | Adult (N = 20) | |
| | | N = | % | N = | % | N = | % |
| Biopsy | | **3** | **9,67** | **2** | **18,18** | **1** | **5,0** |
| | Grade 2 Astrocytoma | 1 | 3,22 | 0 | 0 | 1 | 5,0 |
| | DMG H3K27M | 2 | 6,45 | 2 | 18,18 | 0 | 0,0 |
| Partial Resection | | **21** | **67,74** | **8** | **72,73** | **13** | **65,0** |
| | Low grade Astrocytoma | 1 | 3,22 | 1 | 9,09 | 0 | 0,0 |
| | Grade 2 Astrocytoma | 9 | 29,03 | 1 | 9,09 | 8 | 40,0 |
| | Pilocytic Astrocytoma | 8 | 25,08 | 5 | 45,45 | 3 | 15,0 |
| | DMG H3K27M | 3 | 9,67 | 1 | 9,09 | 2 | 10,0 |
| Near total Resection | | **2** | **6,45** | **1** | **9,09** | **1** | **5,0** |
| | Grade 2 Astrocytoma | 1 | 3,22 | 1 | 9,09 | 0 | 0,0 |
| | Pilocytic Astrocytoma | 1 | 3,22 | 0 | 0,0 | 1 | 5,0 |
| Gross Total Resection | | **5** | **16,13** | **0** | **0** | **5** | **25,0** |
| | Low grade Astrocytoma | 2 | 6,45 | 0 | 0 | 2 | 10,0 |
| | Pilocytic Astrocytoma | 3 | 9,67 | 0 | 0 | 3 | 15,0 |

## 6. Conclusion

In our cohort of spinal cord astrocytomas, we do not demonstrate any statistically significant difference between the radiological characteristics of pediatric and adult populations but we observe some trends: all pediatric PAs occurred at the cervicothoracic junction or the upper cervical region, in contrast most of adult PAs were observed at the thoracic level or below. Secondly, our observations suggest that adults PA are frequently associated with edema but not in the pediatric population. Given the rarity of this type of spinal cord tumor, it is crucial to systematically report such cases to strengthen our databases and improve the diagnosis of pediatric intramedullary astrocytomas.

## Funding

This work was supported by the Fonds Erasme for Medical Research via the Félicien Tomme Convention.

## Author contributions

G.N., L.L., S.I. and D.W.O. designed the study. D.W.O. and G.N. performed the surgeries. The pathological analyses of the tumoral samples were achieved by L.L. and S.I.; L.V. and D.P. reviewed MRI scans and designed the figures. G.N., L.L., R.M., B.A. and C.F. collected all the data. D.M.V. performed statistical analyses. G.N., L.L. and B.A. wrote the manuscript under the supervision of D.W.O. and S.I. All authors contributed to the final version of the manuscript and approved it.

## Declaration of competing interest

The authors declare that they have no known competing financial interests or personal relationships that could have appeared to influence the work reported in this paper.

## References

Bourgouin, P.M., Lesage, J., Fontaine, S., Konan, A., Roy, D., Bard, C., et al., 1998. A pattern approach to the differential diagnosis of intramedullary spinal cord lesions on MR imaging. Am J Roentgenol. june 170 (6), 1645–1649.
Campello, C., Tabouret, E., Chinot, O., 2021. Challenges in diagnosis and management of adult spinal cord gliomas. Rev Neurol (Paris). Maintenant 177 (5), 515–523.
Do-Dai, D.D., Brooks, M.K., Goldkamp, A., Erbay, S., Bhadelia, R.A., 2010. Magnetic resonance imaging of intramedullary spinal cord lesions: a pictorial review. Curr Probl Diagn Radiol. juill 39 (4), 160–185.
Gessi, M., Gielen, G.H., Dreschmann, V., Waha, A., Pietsch, T., 2015. High frequency of H3F3A K27M mutations characterizes pediatric and adult high-grade gliomas of the spinal cord. Acta Neuropathol (Berl). Sept 130 (3), 435–437.
Hachicha, A., Belhaj, A., Karmeni, N., Slimane, A., Bouali, S., Kallel, J., 2021. Intramedullary spinal cord tumors: a retrospective multicentric study. J. Craniovertebral Junction Spine 12 (3), 269.
Houten, JK, Weiner, HL, 2000. Pediatric intramedullary spinal cord tumors: special considerations, 6. https://pubmed.ncbi.nlm.nih.gov/11016739/.
Knafo, S., Aghakhani, N., David, P., Parker, F., 2021. Management of intramedullary spinal cord tumors: a single-center experience of 247 patients. Rev Neurol (Paris). Mai 177 (5), 508–514.
Lebrun, L., Meléndez, B., Blanchard, O., De Nève, N., Van Campenhout, C., Lelotte, J., et al., 2020. Clinical, radiological and molecular characterization of intramedullary astrocytomas. Acta Neuropathol Commun. déc 8 (1), 128.
Louis, D.N., Perry, A., Reifenberger, G., von Deimling, A., Figarella-Branger, D., Cavenee, W.K., et al., 2016. The 2016 world health organization classification of tumors of the central nervous system: a summary. Acta neuropathol (berl). Juin 131 (6), 803–820.
Marrazzo, A., Cacchione, A., Rossi, S., Carboni, A., Gandolfo, C., Carai, A., et al., 2021. Intradural pediatric spinal tumors: an overview from imaging to novel molecular findings. Diagnostics 11 (9), 1710.

Ogunlade, J., Wiginton, J.G., Elia, C., Odell, T., Rao, S.C.. Primary Spinal Astrocytomas: A Literature Review. Cureus [Internet]. 26 juill 2019 [cited 29 mai 2022]; Disponible sur: https://www.cureus.com/articles/17694-primary-spinal-astrocytomas-a-literature-review.

Parker, F., Campello, C., Lejeune, J.P., David, P., Herbrecht, A., Aghakhani, N., et al., 2017. Astrocytomes intramédullaires : analyse rétrospective française multicentrique. Neurochirurgie. nov 63 (5), 402–409.

Seo, H.S., Kim, J.h., Lee, D.H., Lee, Y.H., Suh, S.i., Kim, S.Y., et al., 2010. Nonenhancing intramedullary astrocytomas and other mr imaging features: a retrospective study and systematic review. Am J Neuroradiol. mach 31 (3), 498–503.